

# RGBW LED Mixing Temperature Compensation Method with High Output Consistency

Xuening Liu<sup>a,||</sup>, Changpo Jiang<sup>a,||</sup>, Xiaoke Liu<sup>a</sup>, Zhihao Liu<sup>a,b</sup>, Zhengfei Zhuang<sup>a,b,c,\*</sup>, Min Hu<sup>a</sup>

<sup>a</sup>College of Biophotonics, South China Normal University, Guangzhou, China;

<sup>b</sup>Company of Shida Rayleigh Optoelectronics Technology (Qingyuan), Qingyuan, China;

<sup>c</sup>South China Normal University (Qingyuan) Institute of Science and Technology Innovation, Qingyuan, China;

<sup>||</sup>These authors contributed equally to this work.

\*[zhuangzf@scnu.edu.cn](mailto:zhuangzf@scnu.edu.cn)

## ABSTRACT

This paper proposes a temperature compensation method for RGBW LED mixing based on fast non-dominated sorting genetic algorithm(NSGA-II). The proposed method can achieve compensation for temperature-induced changes in LED correlated color temperature (CCT), color fidelity ( $R_f$ ) and color gamut index ( $R_g$ ) by predicting the spectral power distribution (SPD) at different temperatures. The SPD-temperature model of the RGBW LED light source is established by measuring the spectral power distribution of LEDs at different temperatures. Based on the established model, NSGA-II is used to compensate the mixing temperature of the RGBW LED light source according to the spectral superposition theorem. The experimental results show that the fit of the established temperature-spectral model is  $R^2 > 0.98$ , and the deviation of the compensated mixing results from the initial state of the light source is less than 10K in CCT; the deviation value of  $R_f$  is less than 4% in the range of 2000K-7000K, and less than 2.15% in the range of 3000K-7000K; and the deviation value of  $R_g$  in the range of 2000K-7000K is less than 4.46%.

**Keywords:** LED mixing; temperature compensation; color fidelity; gamut index; NSGA-II;

## 1. Introduction

As lighting technology advances, people are no longer satisfied with using single-colour LEDs for lighting. More people are now inclined to use adjustable LED light sources. Different lighting options can create more comfortable working and living environments. Appropriate lighting can increase people's productivity and lead to better rest<sup>[1-4]</sup>. Compared to traditional light sources, LED light sources have advantages such as smaller size, lower energy consumption and longer life. However, temperature is a critical factor that affects the quality of light sources. Internal heating and extreme external conditions can cause changes in the operating temperature of LEDs, resulting

in parameter deviations and affecting the stability and performance of the light sources<sup>[5-10]</sup>. The advent of adjustable correlated colour temperature (CCT) LED light sources offers a potential solution to the problem of reduced light output quality due to temperature effects.

Currently, the theoretical and experimental research on LED light sources with adjustable CCT is generally divided into three methods: (1) using two white LEDs with different CCT<sup>[11]</sup>; (2) using multiple single-color LEDs<sup>[12-15]</sup>; (3) using a combination of single-color LEDs and white LEDs<sup>[16]</sup>. The first method allows CCT adjustment, and the range of adjustment depends on the selected CCTs of the two white LEDs. The second method allows both CCT and chromaticity coordinate adjustments, with common combinations including RGB, RGBY, and RGBCAL. The advantage of the third method over the second is its ability to reduce the complexity of LED control while achieving a favorable lighting effect.

In this paper, we focus on exploring the optimal lighting performance of RGBW LEDs with the goal of reducing or even eliminating the variations in LED lighting caused by the heating of the LEDs themselves or by external temperature influences. We investigate the proportions of each color LED (R, G, B, and W) in RGBW LED that exhibit similar  $R_f$  and  $R_g$  performance to their initial temperatures within the temperature range of 20°C to 90°C and the CCT range of 2000K to 7000K.

## 2. Experimental description

### 2.1 Multi-Color Light Mixing Principle and Light Source Evaluation

The color of the light source and its ability to accurately reproduce the colors of illuminated objects depends on the spectral power distribution of the light source. The spectral power distribution of a combination of multi-color light sources is the linear sum of their individual spectral power distributions, expressed by the following formula:

$$S_{RGBW} = K_r * S_r + K_g * S_g + K_b * S_b + K_w * S_w \quad (1)$$

White LED light is commonly described in terms of color temperature. Color temperature is defined as the temperature at which a blackbody emits light that matches the color of the light source. Plotting the colors emitted by black bodies at different temperatures in the CIE 1931 color space yields a curve known as the black body locus. However, if the color emitted by the blackbody does not perfectly match the color of the light source—that is, the chromaticity coordinates of the light source do not lie on the blackbody locus—the color temperature is described by the color temperature of the point on the blackbody locus that is closest to the chromaticity coordinates of the light source. This color temperature is called the correlated color temperature. Color temperature and correlated color temperature are typically calculated using empirical formulas proposed by McCamy<sup>[17]</sup> and others, as shown below:

$$CCT = -449n^3 + 3525n^2 - 6823.3n + 5520.33 \quad (2)$$

$$n = \frac{x - 0.3220}{y - 0.1858} \quad (3)$$

The ability of a light source to accurately reproduce the colors of illuminated objects is commonly evaluated using the standardized metric called the CIE (International Commission on Illumination) Color Rendering Index (CRI). The CRI performance of a light source has become an important indicator for evaluating the quality of light sources<sup>[18]</sup>. However, as research on light sources has progressed, the CRI has been found to have some limitations in evaluating certain colors. Therefore, we use the Illuminating Engineering Society (IES) Color Fidelity Index ( $R_f$ ) and Gamut Index ( $R_g$ ) as the evaluation criteria for the illumination performance of light sources<sup>[19]</sup>. The Color Fidelity Index and Gamut Index use 99 color samples, which is more comprehensive than the standard CRI, which typically uses 15 color samples, allowing for a more thorough evaluation of a light source's color performance<sup>[20,21]</sup>. When adjusting a luminaire to achieve the desired correlated color temperature, its  $R_f$  and  $R_g$  performance should be as good as possible to achieve the best lighting effect.  $R_f$  is calculated by determining the difference between the CAM02-UCS coordinates of each CES( $\Delta E_{Jab,i}$ ) under the test source and reference illuminant, and then determining the arithmetic mean of these color differences.  $R_f$  represents the color similarity between the test and reference illuminants and accurately measures the average color fidelity. All color shifts from the reference illuminant are minimal when the  $R_f$  is close to 100. However, light sources with the same  $R_f$  value do not necessarily have the same color performance in the illuminant space. To accurately describe the color performance of the light source, the color shift of the light source must be represented.

The calculation of the Euclidean distance in J'a'b' color space as the standard color difference formula in CAM02-UCS is as follows:

$$\Delta E_{Jab,i} = \sqrt{(J'_{t,i} - J'_{r,i})^2 + (a'_{t,i} - a'_{r,i})^2 + (b'_{t,i} - b'_{r,i})^2} \quad (4)$$

The calculations for  $R_f$  is as follows:

$$R'_f = 100 - 6.73 \left[ \frac{1}{99} \sum_{i=1}^{99} (\Delta E_{Jab,i}) \right] \quad (5)$$

$$R'_f = 100 - 6.73 \left[ \frac{1}{99} \sum_{i=1}^{99} (\Delta E_{Jab,i}) \right] \quad (6)$$

$$R_f = 10 \ln \left[ \exp \left( \frac{R'_f}{10} \right) + 1 \right] \quad (7)$$

$R_g$  is a measure of chroma which is the ratio of the area of the polygon formed by the average coordinate in each hue angle box to the area of the polygon formed by the reference illuminant. The calculation of  $R_g$  is as follows:

$$R_g = 100 * \frac{A_t}{A_r} \quad (8)$$

We evaluate LED mixed-light results from three perspectives: deviation from target color temperature,  $R_f$ , and  $R_g$ . To provide a more intuitive evaluation of the mixed light results, we use a scoring system to quantify the results. The scoring formula is as follows:

$$S = 100 - \frac{CCT}{10} - 2 * (100 - R_f) - |100 - R_g| \quad (9)$$

## 2.2 Establishment of LED Spectral Power Distribution Temperature Model

Due to the inherent characteristics of LEDs, their spectral power distribution (SPD) shifts with temperature<sup>[21]</sup>. In general, for RGB LEDs, the peak wavelengths experience a redshift, and the peak values decrease as the temperature increases. As shown in Figure 1, we tested the spectral power distribution of R, G, B, and W LEDs at 10°C intervals from 20°C to 90°C. It is evident that the red LED is the most affected by temperature, with its peak value at 90°C decreasing by over 60% compared to the peak value at 20°C, and showing a noticeable redshift phenomenon. The blue and green LEDs are less affected compared to the red LED, but their peak values also experience reductions of 20% and 22%, respectively.

To visually represent the changes in spectral power distribution (SPD) of LEDs at different temperatures, it is necessary to mathematically model the SPD of each LED. For single-color LEDs, a Gaussian model is used to simulate their spectral power distribution, with parameters to be determined: peak value, peak wavelength, and full width at half maximum (FWHM). On the other hand, white LEDs typically have two peaks, so a double Gaussian model is used to describe them, with parameters to be determined for both peaks: peak values, peak wavelengths, and FWHMs. Figure 2 shows the measured and fitted spectra of R, G, B, and W LEDs at 20°C. All R2 values are above 0.98, indicating a good representation of the spectral power distribution of the LEDs.

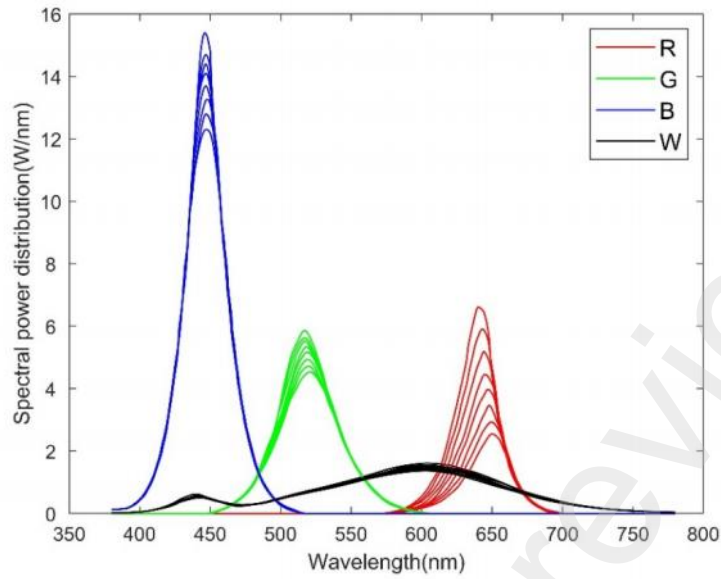


Figure 1. The spectral power distribution of RGBW LEDs at different temperatures

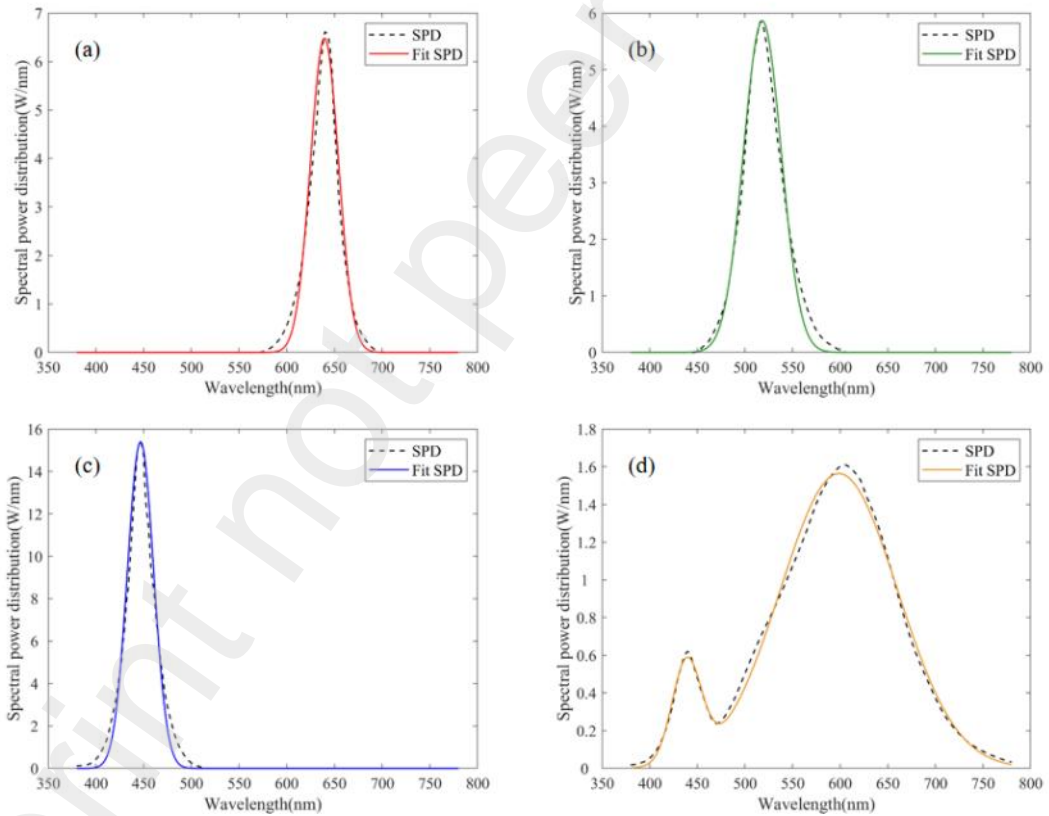


Figure 2. Displays the measured spectra and fitted spectra of LEDs at 20°C for (a) red LED, (b) green LED, (c) blue LED, and (d) white LED.

After establishing the above model, the SPD of LED light sources can be represented by three parameters: peak value, peak wavelength, and full width at half maximum (FWHM). By linearly fitting the peak value, peak wavelength, and FWHM of the Gaussian model at different temperatures, we can obtain the relationship between the SPD and temperature as shown in Equation 10-13. In

the equation, A represents the peak value of the spectral power distribution,  $\lambda_p$  represents the peak wavelength, and  $\Delta\lambda$  represents the FWHM. The subscripts r, g, b, and w represent the corresponding colors of the LED light sources.

$$\begin{bmatrix} A_r \\ \lambda_{pr} \\ \Delta\lambda_r \end{bmatrix} = \begin{bmatrix} 0.0002851 \\ 0.0000357 \\ 0.0001589 \end{bmatrix} \cdot T^2 + \begin{bmatrix} -0.08959 \\ 0.1258 \\ -0.0001369 \end{bmatrix} \cdot T + \begin{bmatrix} 8.304 \\ 637.1 \\ 19.71 \end{bmatrix} \quad (10)$$

$$\begin{bmatrix} A_g \\ \lambda_{pg} \\ \Delta\lambda_g \end{bmatrix} = \begin{bmatrix} -0.000110 \\ -0.000107 \\ 0.0003815 \end{bmatrix} \cdot T^2 + \begin{bmatrix} -0.00780 \\ 0.0456 \\ -0.001601 \end{bmatrix} \cdot T + \begin{bmatrix} 6.018 \\ 517.4 \\ 28.05 \end{bmatrix} \quad (11)$$

$$\begin{bmatrix} A_b \\ \lambda_{pb} \\ \Delta\lambda_b \end{bmatrix} = \begin{bmatrix} -0.000032 \\ 0.000071 \\ 0.000124 \end{bmatrix} \cdot T^2 + \begin{bmatrix} -0.03813 \\ -0.00881 \\ 0.03030 \end{bmatrix} \cdot T + \begin{bmatrix} 16.04 \\ 447 \\ 18.87 \end{bmatrix} \quad (12)$$

$$\begin{bmatrix} A_{w1} \\ \lambda_{pw1} \\ \Delta\lambda_{w1} \\ A_{w2} \\ \lambda_{pw2} \\ \Delta\lambda_{w2} \end{bmatrix} = \begin{bmatrix} -0.0014 \\ 0.0359 \\ 0.0609 \\ -0.0029 \\ -0.0199 \\ 0.0309 \end{bmatrix} \cdot T + \begin{bmatrix} 0.5429 \\ 438.6 \\ 20.57 \\ 1.604 \\ 599.1 \\ 89.14 \end{bmatrix} \quad (13)$$

To validate the reliability of the model, a comparison was made between the calculated and actual SPD. Using the established model, the SPD was calculated for the red LED at 25°C, the green LED at 45°C, the blue LED at 65°C, and the white LED at 85°C. The actual SPD was also measured at these temperatures. The calculated and measured results are shown in Figure 3. The graph shows that the calculated results using the model closely match the actual spectral power distributions, with R2 greater than 0.98.

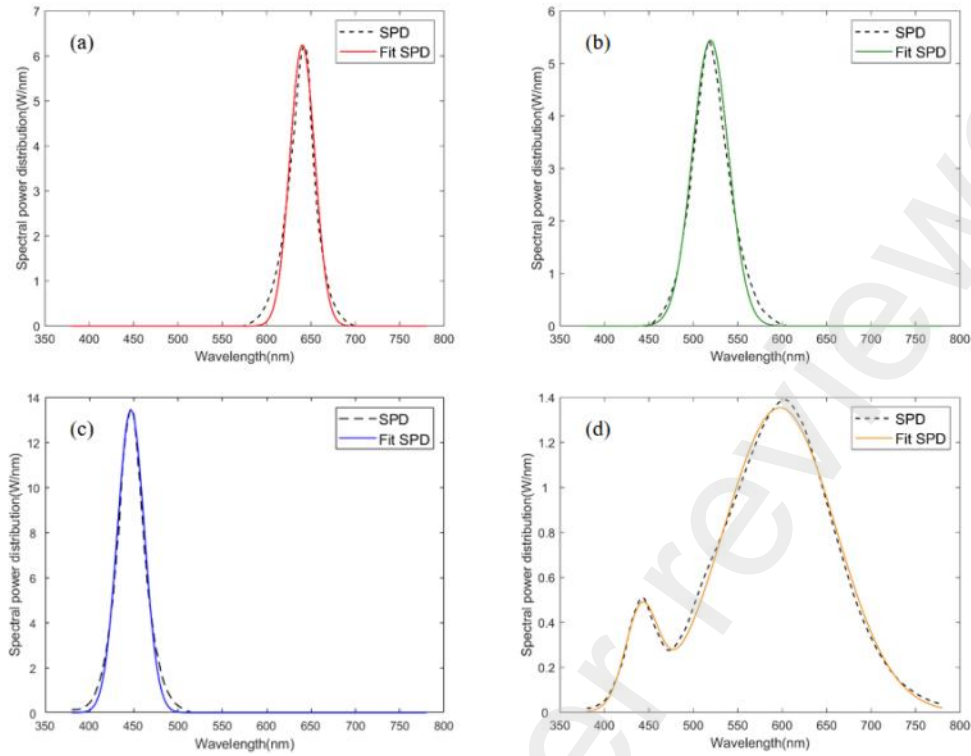


Figure 3. Comparison of the fitted spectra of the temperature spectral model with the tested spectra at different temperatures (a) red LED with 25°C (b) green LED with 45°C (c) blue LED with 65°C (d) white LED with 85°C

### 3. Results and discussion

#### 3.1 Effect of Temperature on Light Mixing Results

The goal of LED temperature compensation is to keep the light output as constant as possible within the target temperature range. First, we need to obtain the light mixing results of the RGBW LED light source at 20 °C . We use PWM to change the duty cycle to realize the control of the different specific gravity of the four LEDs<sup>[23-26]</sup>. Using the spectral power distribution of the RGBW LED light source at 20 °C obtained from the test, we control the duty cycle of the four LEDs and superimpose the spectra, and take the result with the best performance as the initial state. The light source performance in the initial state is shown in Figure 4.

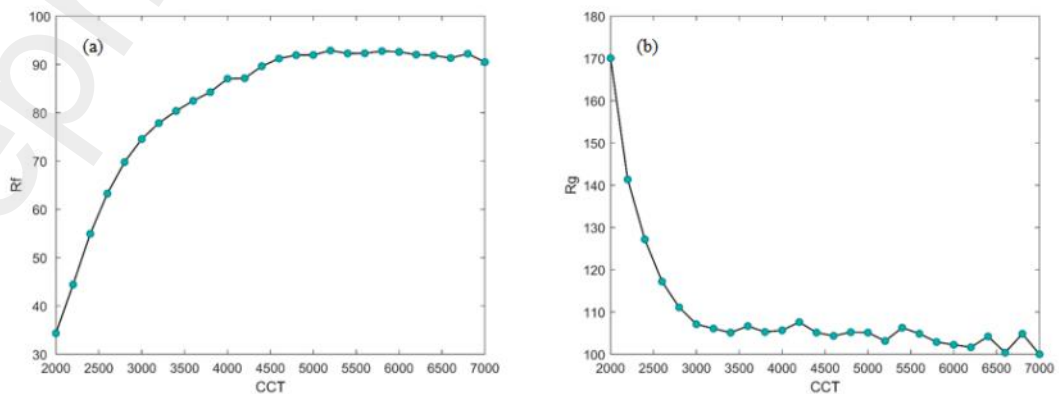


Figure 4. Color performance of RGBW light source in correlated color temperature range of 2000K-7000K

As the temperature increases, using the LED on time directly for light mixing without temperature compensation at the start of the process can result in large variations. The main problem caused by temperature increase is the increase of the color temperature of the light source, and the  $R_g$  and  $R_f$  performance is slightly lower at most color temperatures, as shown in Figure 5. Table 1 shows the  $R_f$  and  $R_g$  at some CCT. Tables 2 and 3 show the CCT,  $R_f$  and  $R_g$  deviations of the RGBW mixing results at 55°C and 85°C. At 55°C compared with 20°C, the maximum deviation of the CCT = 2000K, the deviation value is 333K, the maximum deviation of  $R_f$  = 15.95, the maximum deviation of  $R_g$  = 34.5. At 85°C compared with 20°C, the maximum deviation of CCT = 6500K, the maximum deviation of  $R_f$  = 31.94, and the maximum deviation of  $R_g$  = 53.7.

Table 1. RGBW LED mixing results at 20°C with relative intensities of the four channels

CCT/K	$R_f$	$R_g$	Red	Green	Blue	White
2000	34.3617	170.0625	0.3809	0.0129	0	0.6061
3000	74.5489	107.1144	0.1458	0.0745	0	0.7796
4000	87.0497	105.6701	0.0907	0.1412	0.0358	0.7320
5000	91.9631	105.1416	0.0476	0.1466	0.0839	0.7218
6000	92.5927	102.2622	0.0512	0.2541	0.0834	0.6112
7000	90.4860	100.0014	0.0787	0.3309	0.0975	0.4927

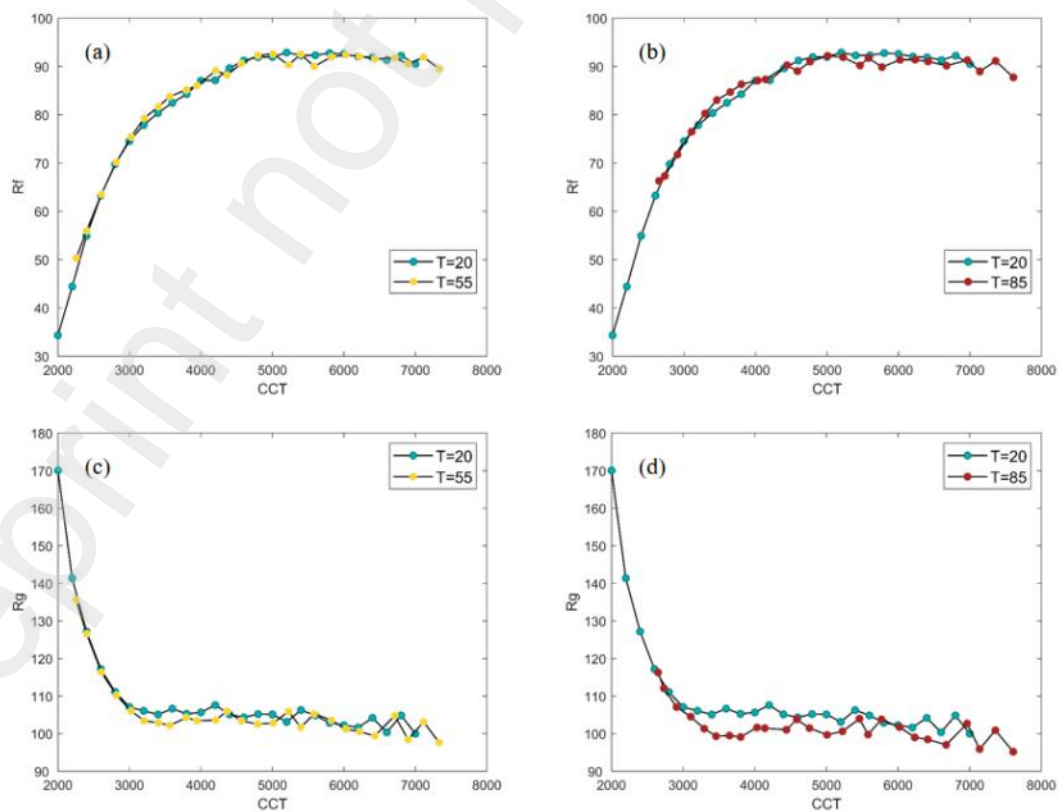


Figure 5. Effect of temperature on the light output of the light source (a) Variation of  $R_f$  at 55°C (b)



Table 2. Variation of  $R_f$  and  $R_g$  at 55°C

CCT/K	CCT deviation/K	$R_f$ deviation	$R_f$ deviation rate	$R_g$ deviation	$R_g$ deviation rate
2000	255	15.9591	46.44%	-34.5027	-20.28%
3000	205	4.6915	6.29%	-3.6654	-3.42%
4000	207	2.0787	2.38%	-2.0318	-1.92%
5000	226	-1.6578	-1.80%	0.7601	0.72%
6000	219	-0.5305	-0.57%	-1.7170	-1.68%
7000	333	-0.9732	-1.08%	-2.3538	-2.35%

Table 3. Variation of  $R_f$  and  $R_g$  at 85°C

CCT/K	CCT deviation/K	$R_f$ deviation	$R_f$ deviation rate	$R_g$ deviation	$R_g$ deviation rate
2000	650	31.94061	92.95%	-53.7363	-31.60%
3000	459	8.479784	11.37%	-7.76715	-7.25%
4000	441	3.206903	3.68%	-4.61825	-4.37%
5000	461	-1.76276	-1.92%	-1.14647	-1.09%
6000	414	-1.56002	-1.69%	-3.77007	-3.69%
7000	607	-2.7493	-3.04%	-4.79731	-4.80%

### 3.2 Temperature compensation of the LED light source

The compensation process is mainly divided into two steps, namely color power compensation and luminance compensation. First, in order to maintain the consistency of the color of the light output as much as possible, the result of temperature compensation is as close as possible to the initial state of the light mixing results. The compensation target is set as the  $R_f$  and  $R_g$  of each color temperature point under 20°C, and the result is to control the relative intensity of the four channels of the light source so that the color performance of the light source is close to the performance under 20°C. Then, the luminance of the light source is adjusted so that the illumination effect of the light source is the same as that at 20°C. However, in some temperature and color temperature, the target brightness could not be achieved due to the attenuation of the peak of the light source, then the light source is set to the closest brightness.

Non-dominated Sorted Genetic Algorithm is commonly used for multi-objective optimization problems. In this paper, the objective is to optimize the deviation,  $R_f$  and  $R_g$  between the mixed color temperature and the target color temperature by controlling each color LED by varying the PWM duty cycle. Figure 6 shows the flow chart of NSGA-2<sup>[27]</sup>. At the beginning of the algorithm, the duty cycles of the four channels are expanded by 1000 times and then converted to binary ones

as gene codes, e.g. if the duty cycle is 0.231, the corresponding code is 0011100111. There are four codes for the duty cycles of the RGBW LEDs, which are concatenated in series to form a set of 40-bit binary codes as genes for storing the information. The crossover, mutation, and variance in the NSGA-II processes in NSGA-II are also performed using this set of genes. It is necessary to scale the set of duty cycles as a whole as shown in Equation 14, when the crossover or mutation process produces a duty cycle greater than 1, that is the binary code is greater than 1111101000.

$$\begin{cases} K_r = K'_r/P \\ K_g = K'_g/P \\ K_b = K'_b/P \\ K_w = K'_w/P \end{cases} \quad (14)$$

$K'$  denotes the duty cycle before scaling,  $K$  denotes the duty cycle after scaling, and  $P$  denotes the maximum duty cycle greater than one.

Set the running parameters of the genetic algorithm, initial population size  $M=30$ , end of evolutionary generations  $G=300$ , crossover probability  $P_c=0.8$ , mutation probability  $P_m=0.1$ . The crossover and mutation probabilities are realized by generating a random number between 0 and 1. If the generated random number is not greater than the value of the probability, the crossover or mutation process is performed. The encoded duty cycle is used as the gene of the individual, and the color temperature deviation of the light mixture and the superiority or inferiority of  $R_f$  and  $R_g$  are used as the adaptation degree of the individual, and the calculation of the adaptation degree is shown in Equation 9.

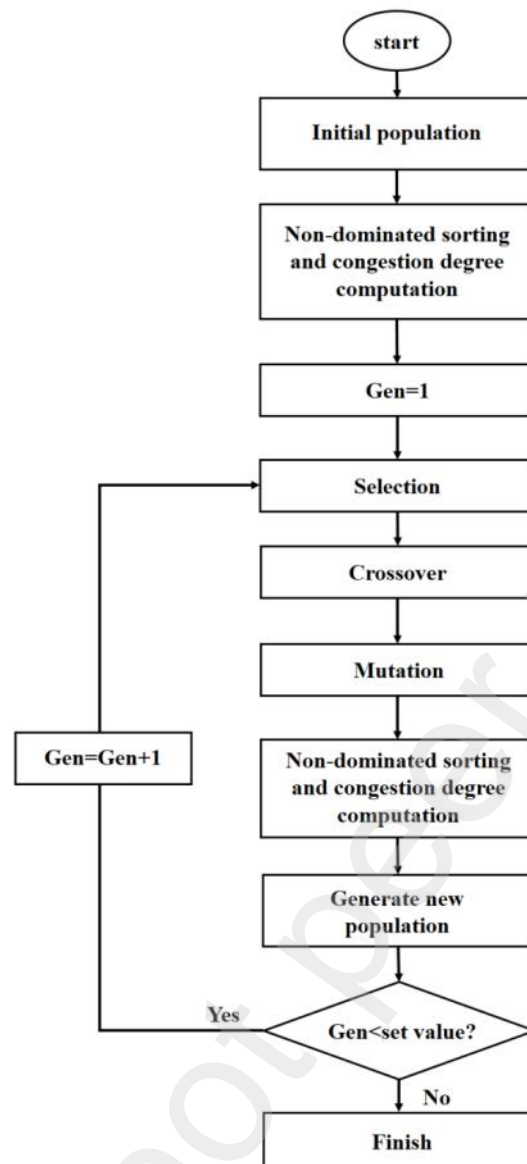


Figure 6. NSGA-II Flowchart

Based on the fitness of the individuals in the initial population, non-dominant sorting and crowding are calculated for all individuals in the population. At this point, the initialization of the population is complete. After the initialization of the population is complete, genetic selection of the population begins until the number of genetic generations reaches the specified number of completed evolutionary generations. At the end of the algorithm, the results are taken as the first level of non-dominated, and the appropriate results in the first level are selected for storage. For the results with large deviation in color temperature but good color performance, they are saved as other parent individuals with similar color temperature to that result to speed up the convergence of the algorithm results. Figure 7 shows the results after color compensation.

For the priority of the optimization target, it is set as the priority of CCT deviation compensation, followed by  $R_f$  compensation and finally  $R_g$  compensation. It can be seen that under this objective, the deviation of the color temperature of the light source from the target color temperature is usually within 10K. The  $R_f$  can also be very close to the performance, and the deviation values are all less than 3. At 55°C, the deviation of the  $R_f$  in the interval of 2000K-7000K is less than 4%, and the deviation of the  $R_f$  in the interval of 3000K-7000K is less than 2.15%. At 85°C, the  $R_f$  deviation is less than 6% in the 2000K-7000K interval and less than 2.21% in the 3000K-7000K interval.  $R_g$  has a lower compensation priority and has a slightly higher deviation than CCT and  $R_f$ , but the deviation values are also usually less than 5. the  $R_g$  deviation is less than 4% at 55°C and less than 4.46% at 85°C. the  $R_g$  deviation is less than 4% at 55°C and less than 4.46% at 85°C. For better results, the population size can be increased and the number of evolutionary generations can be increased. The parameters chosen in this paper allow the calculations to be close to the color performance of the light source at 20°C without taking too much time.

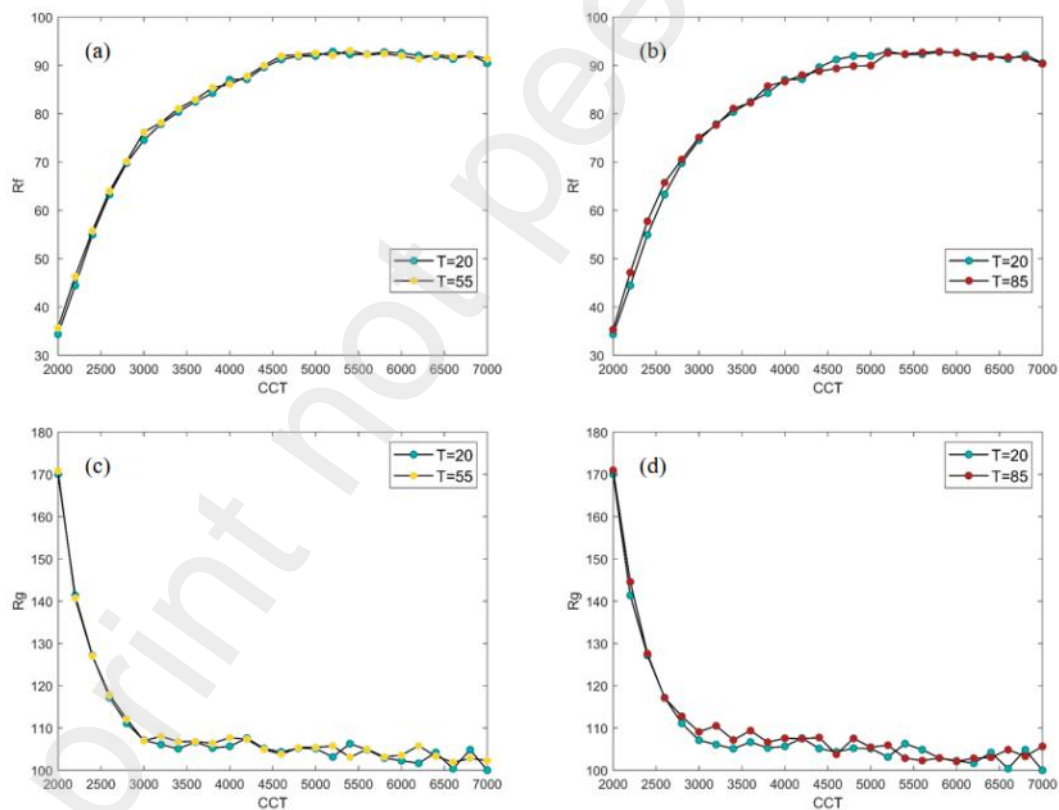


Fig. 7 Color performance of LED light source after color compensation (a) temperature of 55°C for  $R_f$  (b) temperature of 55°C for  $R_g$  (c) temperature of 85°C for  $R_f$  (d) temperature of 85°C for  $R_g$

Since the luminous intensity of the light source is not taken into account when color compensation is performed, it is necessary to make the luminous intensity of the light source consistent with that before color compensation is performed after color compensation is completed.

First of all, we need to calculate the luminous intensity of the light source after the completion of color compensation, using the duty cycle obtained to calculate the SPD of the RGBW LED after mixing, the formula is shown in Equation 1. The luminous intensity of the light source can be further calculated based on the obtained SPD. Then compared to the luminous intensity of the light source before compensation, to maintain the proportion of each light source is unchanged between the mixing duty cycle to amplify or reduce to complete the brightness compensation. Compensation is calculated as follows:

$$\begin{cases} K_r = K'_r * \frac{L'}{L} \\ K_g = K'_g * \frac{L'}{L} \\ K_b = K'_b * \frac{L'}{L} \\ K_w = K'_w * \frac{L'}{L} \end{cases} \quad (15)$$

When the light source temperature is high, a color light source may reach its maximum brightness and still not reach the brightness before compensation. To solve this problem, it is necessary to re-compensate the color at that point, reducing some of the color output in exchange for higher luminous intensity.

#### 4. Conclusion

Multi-color LED mixed lighting future lighting industry trend, based on the lighting effect, control difficulty and cost considerations, the most common multi-color LED mixed lighting solutions on the market for the two-color temperature as well as RGBW. Due to the characteristics of the LED itself, the LED spectral power distribution of different colors will produce different degrees of change when the temperature rises. In this paper, we model the LED spectral power distribution-temperature, and use the NSGA-II algorithm to compensate the spectral temperature of RGBW LEDs based on the spectral superposition theorem, with the goal of making the light output effect of LEDs at different temperatures consistent. The compensation priority for each light output parameter of the light source is color temperature first,  $R_f$  second, and  $R_g$  last. The results show that in the selected group of light sources, the CCT deviation is less than 10K;  $R_f$  deviation value in the range of 2000K-7000K is less than 4%, 3000K-7000K range is less than 2.15%;  $R_g$  deviation value in the range of 2000K-7000K is less than 4.46%. For different application scenarios, different compensation priorities can be controlled to achieve the desired lighting effect.

## References:

- [1] W. Yang, J. Y. Jeon. "Effects of correlated colour temperature of LED light on visual sensation, perception, and cognitive performance in a classroom lighting environment." *Sustainability*. 12(10), 4051. (2020). <https://doi.org/10.3390/su12104051>
- [2] Z. Huang, W. Chen, Q. Liu, Y. Wang. "Towards an optimum colour preference metric for white light sources: a comprehensive investigation based on empirical data. " *Optics Express*. 29(5), 6302-6319. (2021). <https://doi.org/10.1364/OE.413389>
- [3] D. Qi, W. Cai, W. Shi, L. Hao, and M. Wei. "A proposed lighting-design space: circadian effect versus visual illuminance." *Building and Environment*. 122(17), 287-293. (2017). <https://doi.org/10.1016/j.buildenv.2017.06.025>.
- [4] T. Aderneuer, O. Stefani, O. Fernández, C. Cajochen, and R. Ferrini. "Circadian tuning with metameric white light: Visual and non-visual aspects. " *Lighting Research & Technology*. 53(6), 543-554. (2021). <https://doi.org/10.1177/1477153520976934>
- [5] M. G. Figueiro, and M. S. Rea. "Office lighting and personal light exposures in two seasons: Impact on sleep and mood. " *Lighting Research & Technology*. 48(3), 352-364. (2016). <https://doi.org/10.1177/1477153514564098>
- [6] I. Plotog, and M. Vladescu. "Power LED efficiency in relation to operating temperature." *Advanced Topics in Optoelectronics, Microelectronics, and Nanotechnologies VII*. 9258, 652-657. (2015). <https://doi.org/10.1117/12.2072276>
- [7] S. K. Ng, K. H. Loo, Y. M. Lai, and K. T. Chi. "Color control system for RGB LED with application to light sources suffering from prolonged aging." *IEEE Transactions on Industrial Electronics*. 61(4), 1788-1798. (2013). <https://doi.org/10.1109/TIE.2013.2267696>
- [8] M. R. Quispe, F. M. A. Oscco, M. J. Horn, and M. M. Gómez. "Influence of the temperature of a white LED on its lighting characteristics." *Journal of Physics: Conference Series*. 2538(1), 012009. (2023). <https://doi.org/10.1088/1742-6596/2538/1/012009>
- [9] C. D. Tong, G. Y. Li, X. Zheng, C. B. Chen C. B., Z. J. Ke, Wu, R. X., and W. J. Guo. "Luminous Properties of Red, Green, and Blue Micro-LEDs and the Impacts on Color Gamut." *IEEE Transactions on Electron Devices*. 70(4), 1733-1738. (2023). <https://doi.org/10.1109/TED.2023.3247362>.
- [10] F. Reifegerste, and J. Lienig. "Modelling of the temperature and current dependence of LED spectra." *Journal of Light & Visual Environment*. 32(3), 288-294. (2008).
- [11] J. O. Kim, J. U. N. G. Byung-Joon, and R. Y. U. Uh-Chan. "A Simulation Study on Color Rendering Characteristics of CCT-tunable LED Lightings Composed of WW-LEDs and CW-LEDs in Tracing the Planckian Locus by Adding Single-wavelength LEDs." *New Physics: Sae Mulli*. 72(1), 33-41. (2022). <http://dx.doi.org/10.3938/NPSM.72.33>
- [12] X. Qu, S. C. Wong, and K. T. Chi. "Temperature measurement technique for stabilizing the light output of RGB LED lamps." *IEEE Transactions on Instrumentation and measurement*. 59(3), 661-670. (2009). <https://doi.org/10.1109/TIM.2009.2025983>
- [13] L. Zhu, B. Yao, L. Deng, Y. Yang, G. Wang, C. Gu, L. Xu. "Evaluation of gamut enhancement in yellow regions and a choice of optimal wavelength for a RGBY four-primary laser display system." *Optics Express*. 30(21), 38938-38952. (2022). <https://doi.org/10.1364/OE.468131>
- [14] X. Zhan, W. Wang, H. S. H. Chung. "A novel color control method for multicolor LED systems

- to achieve high color rendering indexes." *IEEE Transactions on Power Electronics*. 33(10), 8246-8258. (2017). <https://doi.org/10.1109/TPEL.2017.2785307>
- [15] A. Eissfeldt, and T. Q. Khanh. "Algorithm for real-time colour mixing of a five-channel LED system while optimising spectral quality parameters." *Lighting Research & Technology*. 54(6), 563-575. (2022). <https://doi.org/10.1177/14771535211058096>
- [16] M. Tanaka, T. Horiuchi, and S. Tominaga. "Color control of a lighting system using RGBW LEDs." *Color Imaging XVI: Displaying, Processing, Hardcopy, and Applications*. 7866, 256-264. (2011). <https://doi.org/10.1117/12.872374>
- [17] C. S. McCamy. "Correlated color temperature as an explicit function of chromaticity coordinates." *Color Research & Application*. 17(2), 142-144. (1992).
- [18] C. Wu, Z. Liu, Z. Yu, X. Peng, Z. Liu, X. Liu, and Y. Zhang. "Phosphor-converted laser-diode-based white lighting module with high luminous flux and color rendering index." *Optics Express*. 28(13), 19085-19096. (2020). <https://doi.org/10.1364/OE.393310>
- [19] M. P. Royer. "Tutorial: Background and guidance for using the ANSI/IES TM-30 method for evaluating light source color rendition." *Leukos*. 18(2), 191-231. (2022).
- [20] M. P. Royer. "Comparing measures of average color fidelity." *Leukos*. 14(2), 69-85. (2018). <https://doi.org/10.1080/15502724.2017.1389283>
- [21] X. Qu, S. C. Wong, and K. T. Chi "Color control system for RGB LED light sources using junction temperature measurement." *IECON 2007-33rd Annual Conference of the IEEE Industrial Electronics Society*. IEEE, 1363-1368. (2007).
- [22] F. Zhang, H. Xu, and Z. Wang, "Optimizing spectral compositions of multichannel LED light sources by IES color fidelity index and luminous efficacy of radiation." *Applied optics*. 56(7), 1962-1971. (2017). <https://doi.org/10.1364/AO.56.001962>
- [23] H. Ren, S. Li, R. Sun, and Z. Su. "Study on LED Color Mixing for Stage Lighting Based on Locus Fitting of Blackbody." *2017 International Conference on Computer Technology, Electronics and Communication (ICCTEC)*. IEEE, 295-299. (2017). <https://doi.org/10.1109/ICCTEC.2017.00070>
- [24] Q. Wang, J. Ding, D. Ma, Y. Cheng, L. Wang, and F. Wang. "Manipulating Charges and Excitons within a Single - Host System to Accomplish Efficiency/CRI/Color - Stability Trade - off for High - Performance OWLEDs." *Advanced Materials*. 21(23), 2397-2401. (2009). <https://doi.org/10.1002/adma.200803312>
- [25] M. Lukovic, V. Lukovic, I. Belca, B. Kasalica, I. Stanimirovic, and M. Vicic. "LED-based Vis-NIR spectrally tunable light source-the optimization algorithm." *Journal of the European Optical Society-Rapid Publications*. 12,1-12. (2016). <https://doi.org/10.1186/s41476-016-0021-9>
- [26] X. Zhan, W. Wang, H. Chung. "A neural-network-based color control method for multi-color LED systems." *IEEE Transactions on Power Electronics*. 34(8), 7900-7913. (2018). <https://doi.org/10.1109/TPEL.2018.2880876>
- [27] K. Deb, S. Agrawal, A. Pratap, T. Meyarivan. "A fast elitist non-dominated sorting genetic algorithm for multi-objective optimization: NSGA-II." *Parallel Problem Solving from Nature PPSN VI*. Springer Berlin Heidelberg, 849-858. (2000).